Systematic study of proton-induced spallation reactions with microscopic and phenomenological models

A. Assimakopoulou, G. A. Souliotis, N. Nicolis, M. Veselsky, A. Bonasera

Systematic study of proton-induced spallation reactions with microscopic and phenomenological models

A. Assimakopoulou[1], G.A. Souliotis[1,*], N. Nicolis[2],
M. Veselsky[3] and A. Bonasera[4,5]

[1] *Laboratory of Physical Chemistry, Department of Chemistry, National and Kapodistrian University of Athens, Athens 15771, Greece*

[2] *Department of Physics, The University of Ioannina, Ioannina 45110, Greece*

[3] *Institute of Physics, Slovak Academy of Sciences, Bratislava 84511, Slovakia*

[4] *Cyclotron Institute, Texas A & M University, College Station, Texas, USA*

[5] *Laboratori Nazionali del Sud, INFN, Catania, Italy*

Abstract

Proton induced spallation reactions on ^{238}U, ^{208}Pb, ^{181}Ta and ^{197}Au targets at high energies were investigated using the microscopic Contrained Molecular Dynamics (CoMD) model and the phenomenological models INC and SMM. We have calculated the total fission cross sections, the ratio fission cross section to residue cross section, the mass yield curves and the excitation energy after the intranuclear cascade using the CoMD model and the INC/SMM phenomenological models. We made a comparison between the models and the experimental data from the literature. Our calculations showed satisfactory agreement with available experimental data and suggest further improvements in the models. Our study with the CoMD code represents the first complete dynamical description of the spallation process with a microscopic code based on an effective nucleon-nucleon interaction.

1 Introduction

Spallation reactions induced by high-energy protons are of importance for fundamental research and technical applications in nuclear physics, as for instance, medical physics applications and nuclear-reactor technologies. The most important applications of these reactions are the spallation neutron

---

[1] * Corresponding author. Email: soulioti@chem.uoa.gr

sources [1,2], energy production techniques based on accelerator driven systems (ADS) [3,4], transmutation of radioactive waste [5–7] and radiation shield design for accelerators and cosmic devices [8]. Other applications are the production of radioactive ion-beams [9], in ISOL-type facilities and radiopharmacological production [10,11]. All these applications require the total fission cross section to be known with high accuracy in a wide proton energy range.

Many efforts have been made in providing experimental data on interactions in the energy range (100 –1000 MeV) protons and neutrons with targets that are used in the various applications. Because of the variety of target nuclei and the wide range of energy of the beam particles, theoretical models and nuclear-reaction codes are needed.

Since the available experimental data on spallation reactions are rather poor and fragmentary, an experimental and theoretical work started at GSI Darmstadt [12]. In particular, the production of individual nuclides from charged-particle induced spallation reactions were measured, using the inverse kinematics technique with the high resolution magnetic spectrometer FRS. Also improved codes, such as INCL [13], were developed. However, there are still uncertainties concerning measured total fission cross sections and other observables. Most of the models describe the spallation reaction as a two-stage process. A code that has been extensively used is the Liege Intranuclear Cascade Model, INCL++ [14], which describes the first (fast) stage of the intranuclear cascade. Another code that describes the intranuclear cascade is the Monte Carlo simulation code CRISP [17]. The second stage is described by an evaporation-fission model like GEMINI,GEMINI++ [15], ABRA07 [16] or the generalized evaporation model (GEM) [18]. Moreover, the Statistical Multifragmentation Model (SMM) [20–24] is a deexcitation code which combines the compound nucleus processes at low energies and multifragmentation at high energies.

In the present work we used the CoMD model, which is described in the references [25–29] and the phenomenological models INC [19] and SMM. With the CoMD model we obtained (p,f) cross sections, mass yield curves, fission to residue cross sections, and neutron multiplicities for the targets ^{238}U, ^{208}Pb, ^{181}Ta at 200, 500 ,1000 MeV and ^{197}Au at 800 MeV. We chose these targets because they are important especially for accelerator-driven systems (ADS). For example tantalum alloys and leadbismuth eutectic are optimum materials for the construction of spallation neutron sources. In our work, we compared our CoMD calculations with experimental data taken from refs. [31,32,34,35,37–40]. With the INC model we calculated the excitation energy of ^{208}Pb nucleus after the intranuclear cascade and with the combination of INC/SMM models we obtained the mass distributions of ^{208}Pb and ^{238}U targets as well as the total fission cross sections.

2   Theoretical Model

The Constrained Molecular Dynamics (CoMD) code is based on the gereral approach of molecular dynamics as applied to nuclear systems [29,30]. The nucleons are assumed to be localized gaussian wavepackets in coordinate and momentum space. A simplified effective nucleon-nucleon interaction is implemented with a nuclear-matter compressibility of K=200 (soft EOS) with several forms of the density dependence of the nucleon-nucleon symmetry potential. In addition, a constraint is imposed in the phase space occupation for each nucleon, restoring the Pauli principle at each time step of the collision. Proper choice of the surface parameter of the effective interaction was made to describe fission.

In the calculations of the present work, the CoMD code was used essentially with its standard parameters. The soft density-dependent isoscalar potential was chosen (K=200). For the isovector part, two forms were used: the "standard" symmetry potential [red (solid) lines] and the "soft" symmetry potential [blue (dotted) lines] in the figures that follow. These forms correspond to a dependence of the symmetry potential on the 1 and the 1/2 power of the density, respectively [26]. The surface term of the potential was set to zero to describe fission. For a given reaction, a total of approximately 5000 events were collected. For each event, the impact parameter of the collision was chosen in the range b = 0–7 fm, following a triangular distribution. Each event was followed up to 15000 fm/c and the phase space coordinates were registered every 100 fm/c. At each time step, fragments were recognized with the minimum spanning tree method [25,28] and their properties were reported. Thus, information on the evolution of the fissioning system and the properties of the resulting fission fragments were obtained. In this way, the moment of scission of the deformed heavy nucleus could be determined. We allowed 5000 fm/c after scission for the nascent fission fragments to deexcite and we reported and analyzed their properties. We mention that the effective nucleon-nucleon interaction employed in the code has no spin dependence and thus the resulting mean field has no spin-orbit contribution. We are exploring possibilities of adding such a dependence on the potential to give us the ability to adequately describe the characteristics of fission at lower excitation energies i.e. $E^* < 50$ MeV.

3   Results and Comparisons

The present work was based on the use of the microscopic CoMD model and the combination INC and SMM models in order to simulate the p-induced spallation reactions at intermediate and high enegies on heavy targets (^{238}U,^{208}Pb,

^{181}Ta and ^{197}Au) . In the following, we present the excitation energy distribution of ^{208}Pb nucleus, the mass yield curve of the reaction p (1000 MeV) + ^{208}Pb and p (1000 MeV) + ^{238}U, the total fission cross section of ^{208}Pb and finally the ratio fission to residue cross section for the targets ^{238}U, ^{208}Pb, ^{181}Ta and ^{197}Au. We compare our theoretical calculations with available experimental data as it is shown on the corresponding figures.
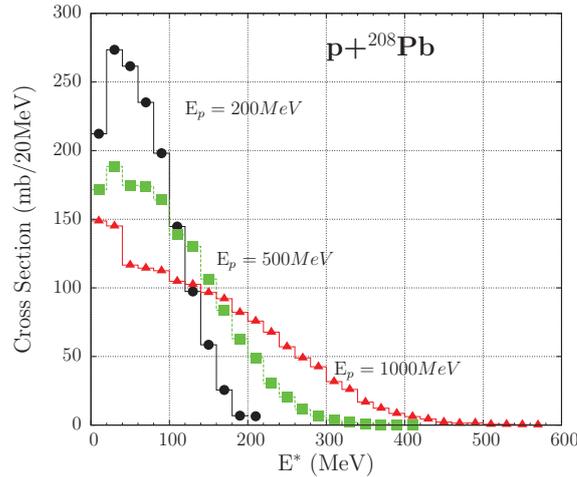

Fig. 1. (Color online) Excitation energy distribution as a function of the cross section for ^{208}Pb target at 200, 500 and 1000 MeV calculated with the INC model. The solid circles represent the E_p=200 MeV, the solid squares represent the energy beam at 500 MeV and the solid triangles represent the energy beam at 1000 MeV.

In Fig. 1, we present the excitation energy distribution as a function of the cross section after the intranuclear cascade for the ^{208}Pb target at 200, 500 and 1000 MeV, calculated with the INC model. We also calculated the mean excitation energy, which is about 55 MeV at E_p=200 MeV, about 85 MeV at E_p=500 MeV and about 130 MeV at E_p=1000 MeV.

In Fig. 2, we show the mass distribution of proton induced spallation of ^{208}Pb at 1000 MeV. We compare our theoretical results with the experimental data of [37], which are indicated with black triangles. The (red) solid circles with the solid line represent the standard symmetry potential from the CoMD code while the grey (green) open circles represent the INC calculations. On this figure we distinguish two regions of fragments. One region has the heavy residues with larger mass numbers, close to the target and the other region has the fission fragments with the smaller mass numbers. We can observe, that in the region with the fission fragments, the CoMD calculations and the INC/SMM calculations are in overall agreement with the experimental data. In the heavy residues region, the CoMD calculations and the INC/SMM calculations have a discrepancy with the data.

In Fig. 3 we display the mass distribution of proton induced spallation of ^{238}U at 1000 MeV. We compare our theoretical results with the experimental data

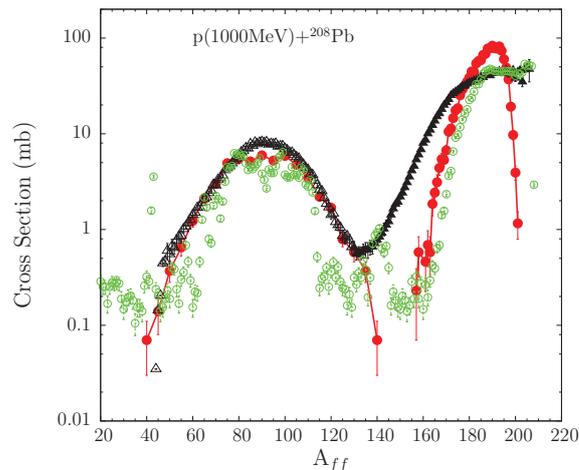Fig. 2. (Color online) Normalized mass distributions of fission fragments and heavy residues for p (1000 MeV) $+^{208}$Pb. Experimental data: solid (black) trinagles [37]. The solid (red) circles represent the CoMD calculations and the open (green) circles the INC/SMM calculations.
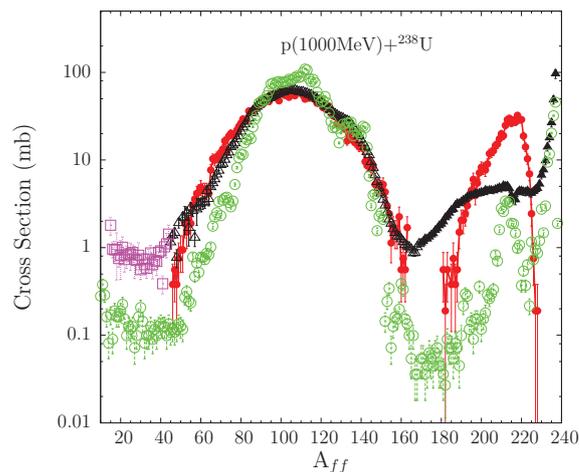

Fig. 3. (Color online) Mass distributions of fission fragments and heavy residues for the reaction p(1000 MeV) $+ {}^{238}$U. Experimental data: open (pink) squares [46], open (black) triangles [35] and solid (black) triangles [47]. The solid (red) circles represent the CoMD calculations and the open (green) circles the INC/SMM calculations.

of [35,36,46,47]. The (red) solid circles represent the standard symmetry potential from the CoMD code, the (green) open circles represent the INC/SMM calculations and the experimental data are represented with the (pink) open squares, open (black) triangles and solid (black) triangles. The green points represent the Intermediate Mass Fragments. Similarly, we have two regions of fragments, the heavy residues region and the fission fragment region. We can observe, that in the fission fragments region, the CoMD calculations and the INC/SMM calculations are in overall agreement with the experimental data and in the heavy residues region there is a discrepancy between the data and our theoretical results.
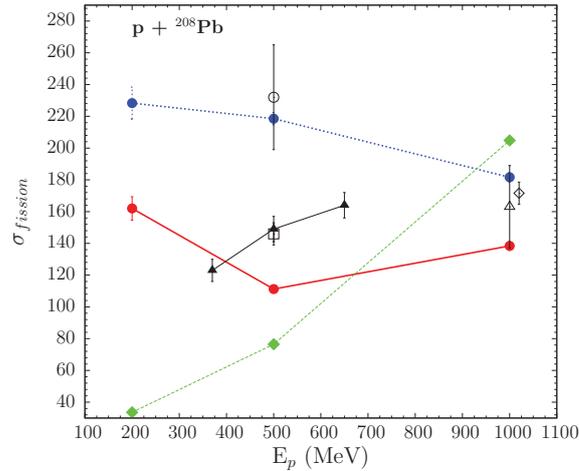
Fig. 4. (Color online) Fission cross section as a function of the proton energy at 200, 500 and 1000 MeV for ^{208}Pb target. Experimental data: solid triangle [43], open triangle [37], open square [44], open circle [44], open circle [34] and open diamond [33]. CoMD calculations: standard symmetry potential full (red) circles with solid line and soft symmetry potential full (blue) circles with dashed line. INC/SMM calculations: solid (green) diamonds.

In Fig. 4, we present the total fission cross sections calculated with the CoMD code and the INC/SMM models for ^{208}Pb target at 200, 500, 1000 MeV as a function of the proton energy. Our calculations are compared with experimental data and we also present predictions obtained with the systematics established by Prokofiev [33]. The (red) points with the solid line represent the standard symmetry potential and the (blue) points with the dashed line the soft symmetry potential from the CoMD code, while the (green) solid diamonds present the INC/SMM calculations. At 1000 MeV our calculations are in some agreement with the systematics of Prokofiev [33] and the measurements of T. Enqvist et al.[37]. At 500 MeV the CoMD calculations appears to be in moderate agreement with the data by B. Fernandez et al. [34], J.L. Rodriguez et al. [43] and with K.-H. Schmidt et al. [44], while the INC/SMM calculations underestimate both the data and CoMD calculations. Finally, at 200 MeV there is a large dicrepancy between the CoMD and the INC/SMM calculations.

In figure 5, we show the ratio of the fission cross section to the heavy-residue cross section as a function of the proton energy for ^{238}U, ^{208}Pb and ^{181}Ta, calculated with the CoMD code and INC/SMM models at 200, 500 and 1000 MeV and ^{197}Au at 800 Mev. We compare the calculations with the indicated experimental data, which are presented with black points. The (red) solid points with the solid line represent the standard symmetry potential and the (blue)open points with the dashed line the soft potential from the CoMD code, while the grey (green) triangles present the INC/SMM calculations for ^{208}Pb target and the grey (yellow) point the INC/SMM calculations for 197Au at
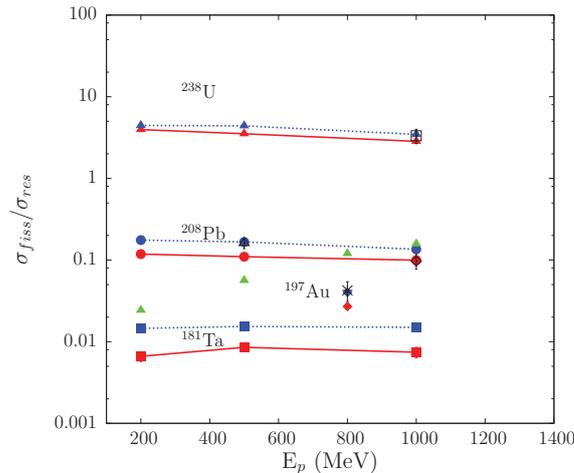
Fig. 5. (Color online) Ratio of the fission to residue cross section as a function of the proton energy at 200, 500 and 1000 MeV for the targets ^{238}U, ^{208}Pb, ^{181}Ta and ^{197}Au at 800 MeV. Experimental data: open square [35], open triangle [34], rhombus [37], star [38,39] CoMD calculations: standard symmetry potential full (red) points and soft symmetry potential full (blue) points. INC/SMM calculations for ^{208}Pb target: solid (green) triangles.

800 MeV. At first, we can observe that the ratio of ^{238}U is about 8, which of course indicates that it is a high fissile nucleus. This value means that it has much higher possibility to undergo fission than evaporation. We notice also that the CoMD calculations at 1000 MeV are in good agreement with the data of Bernas et al. [35]. The ratio of fission cross section to residue cross section for ^{208}Pb calculated with the CoMD calculations is about 10%. This indicates that the lead target has a modest fissility. It appears that our calculations are in good agreement with the data of Fernandez et al. [34] at 500 MeV, especially our results with the soft symmetry potential. At 1000 MeV, the CoMD calculations with the standard potential are in good agreement with the data of Enqvist et al. [37]. Next, we present the ratio of ^{197}Au at 800 MeV which is 4%. This suggests an intermediate fissility in relation with tantalum and lead. We also compare our results with experimental data [38,39] for ^{197}Au, which are displaced by 20 MeV for viewing purposes. The CoMD calculations with the soft symmetry potential are in very good agreement with the data. For ^{181}Ta, the ratio is only about 1%, as calculated from the CoMD. This low value suggests that ^{181}Ta has a low fissility and thus, has a tendency to undergo mostly evaporation. In general, we observe that the CoMD calculations with the soft potential are higher than the standard potential.

4 Discussion and Conclusions

In the present work we employed the semi-classical microscopic code CoMD to describe proton induced spallation in a variety of energies on ^{238}U, ^{208}Pb, ^{197}Au and ^{181}Ta nuclei. In addition we used the phenomenological models INC and SMM in the standard two-stage scenario. In our study we chose these nuclei because of the availability of recent literature data and because of their significance in current applications of spallation. We observe that the fission of ^{208}Pb and ^{238}U target is symmetric due to the high excitation energy at which the shell effects are fully washed out [48]. Also we reproduced well the total fission cross sections and the ratio of fission over residue cross sections. In general, we point out that the CoMD code gives results that are not dependent on the specific dynamics being explored and, thus, offers valuable predictive power for the different modes of fission. A comparison of our calculations with some of the available experimental data from the literature showed satisfactory agreement. It appears that the microscopic code CoMD is able to describe the complicated N-body dynamics of the fission/spallation process. In closing, we suggest the systematic study of the above observables of spallation reactions and further comparison with experimental data. Moreover, apart from the microscopic CoMD code, we used the phenomenological models INC and SMM. Both the microscopic CoMD and the two phenomenological models decribe well the fission process, while it seems that the spallation/evaporation process they cannot describe it well. We are planning to use the statistical model MECO for better description of the evaporation process and we will compare the models with each other.

5 Acknowledgements

6 REFERENCES

References

[1] K.N Clausen, in Proceedings of the 16th Meeting of the International Collaboration on Advanced neutron Sources, ICANS-XVI, edited by G.Mank

and H.Conrad (Forshungszentrum Jlich GmbH,Jlich, Germany, 2003), Vol. 1,2 and 3.

[2] The European Spallation Source Study, The ESS Technical Study, Vol.III, 1996, Report ESS-96-53-M.

[3] H. Daniel, Y. Petrov, Subcritical fission reactor driven by the low power accelerator, Nucl. Instrum. Methods Phys. Res.**A 373**, (1), 131-134 (1996)

[4] H. Nifenecker, S. David, J. Loiseaux, A. Giorni, Prog. Part. Nucl. Phys. **43**, 683-827 (1999)

[5] C.D. Bowman, Ann. Rev. Nucl. Part. Sci. **48**, 505 (1998).

[6] C. Rubbia et al.,CERN report,1995, CERN/AT/95-44(ET).

[7] H. Nifenecker et al., Nucl. Instrum. Methods **A 463**, 428 (2001)

[8] A.J. Koning, J.-P.Delaroche, and O. Bersillon, Nucl. Instrum. Methods Phys. Res. **A 414**, 49 (1998).

[9] M. Lewitowicz, J. Phys.:Conf. Ser.**312**, 052014 (2011)

[10] W. Uyttenhove, P. Baeten, G.V. den Eynde et al., Ann. Nucl. Energy **38** (7), 1519-1526 (2011)

[11] K. Abbas, S. Buono, N. Burgio et al., Nucl.Instrum. Methods Phys. Res.**A 601** (3), 223-228 (2009)

[12] https://www-win.gsi.de/charms.

[13] A. Boudard, J. Cugnon, S. Leray, and C. Volant, Phys. Rev. **C 66**, 044615 (2002).

[14] A. Boudard et al., Phys. Rev. **C 87**, 014606 (2013)

[15] D. Mancusi, R.J. Charity, J. Cugnon, Phys. Rev. C **C 82**, 044610 (2010)

[16] A. Kelic et al., in: D. Filges et al.(Eds.), Proceedings of the Joint ICTP-IAEA Advanced Workshop on Model Codes for Spallation Reactions, ICTP Trieste, Vienna, Italy, 4-8 February 2008,IAEA report INDC(NDS)-530,2008,p.181.

[17] A. Deppman et al., Phys.Rev. **C 88**, 024608 (2013)

[18] S. Furihata, Nucl.Instrum. Methods **B 171**, 251 (2000)

[19] Y. Yariv, Z. Fraenkel, Phys. Rev. C 24, 488-494 (1981)

[20] N. Eren, N. Buyukcizmeci, R. Ogul, and A.S. Botvina, Eur. Phys.J. **A 49**, 48 (2013)

[21] J. Bondorf et al., Phys. Rep. **257**, 133 (1995)

[22] A.S. Botvina and I. N. Mishustin, Phys Rev. **C 63**, 061601 (2001)

[23] G.A. Souliotis et al. Phys. Rev. **C 75**, 011601 (2007)

[24] N. Buyukcizmeci, R. Ogul, and A. S. Botvina, Eur. Phys. J. **A 25**, 57 (2005)

[25] M. Papa et al., Phys. Rev. **C 64**, 024612 (2001).

[26] M. Papa, Phys. Rev. **C 87**, 014001 (2013).

[27] N. Vonta, G. A. Souliotis, M. Veselsky, A. Bonasera, Phys. Rev. **C 92**, 024616 (2015).

[28] M. Papa et al, J. Comp. Phys. **208**, 403 (2005).

[29] J. Aichelin, Phys. Rep. **202**, 233 (1991).

[30] A. Bonasera, F. Gulminelli, J. Molitoris, Phys. Rep. **243**, 1 (1994).

[31] J.L. Rodriguez-Sanchez, J. Benlliure et al., Phys. Rev. **C 91**, 064616 (2015).

[32] L. Audouin et al., Nucl. Phys. **A 768**, 1-21 (2006).

[33] A. V. Prokofiev, Nucl. Instrum. and Methods in Phys. Res. **A 463**, 557-575 (2001)

[34] B. Fernandez et al., Nucl. Phys. **A 747**, 227-267 (2005).

[35] M. Bernas et al., Nucl. Phys. **A 725**, 213-253 (2003).

[36] M. Bernas et al., Nucl. Phys. **A 765**, 197 (2006).

[37] T. Enqvist et al., Nucl. Phys.**A 686**, 481-524 (2001).

[38] J. Benlliure, P. Armbruster et al., Nucl. Phys. **A 700**, 469-491 (2002).

[39] F. Rejmund et al., Nucl. Phys. **A 683**, 540-565 (2001).

[40] S. Leray et al., Phys. Rev.**C 65**, 044621 (2002).

[41] J. Benlliure, P. Armbruster et al., Nucl. Phys. **A** 683, 513-539 (2001)

[42] Y. Ayyad, J. Benlliure et al., Phys. Rev. **C 89**, 054610 (2014)

[43] J. L. Rodriguez et al., Phys. Rev. **C 90**, 064606 (2014)

[44] K. -H. Schmidt et al., Phys. Rev. **C 87**, 034601 (2013)

[45] A. A. Kotov et al. Phys. Rev.**C 74**, 034605 (2006)

[46] M. V. Ricciardi et al., Phys. Rev.**C 73**, 014607 (2006)

[47] J. Taieb et al., Nucl. Phys. **A 724**, 413-430 (2003)

[48] A. Chaudhuri et al., Phys. Rev. C 91, 044620 (2015)